

Factors influencing the crushing strength of some Aegean sands

Yusuf Erzin · A. Patel · D. N. Singh ·
M. G. Tiga · I. Yilmaz · K. Srinivas

Received: 7 August 2011 / Accepted: 20 February 2012 / Published online: 6 April 2012
© Springer-Verlag 2012

Abstract Engineering properties of sands mainly depend on the integrity of the particles, which in turn has a strong bearing on their crushing strength. Seven different Aegean sands were tested for mineralogy, particle shape, size and specific gravity and the influence of aspect ratio, particle composition, particle shape and size on the crushing strength was examined. As the Aegean sands have a small range of sphericity and roundness, crushing strength tests were also performed on five Anatolian sands. A multiple regression analysis was carried out and an equation proposed to determine the crushing strength value of the Aegean sands. The computed values were found to be in good agreement with those obtained from the experimental investigations. It is concluded that the equation is sufficiently accurate to be a useful, time- and cost-effective way of obtaining crushing strength estimations at the preliminary stage of site investigations.

Keywords Aegean sands · Anatolian sands · Crushing strength · Particle morphology · Sphericity · Roundness

Résumé Les propriétés géotechniques de sables dépendent principalement de l'intégrité des particules qui est fortement en rapport avec leur résistance à l'écrasement. Sept sables égéens différents ont été analysés quant à la nature minéralogique des grains, la forme et la taille de particules et leur densité. Les influences de la composition des particules, de leur forme et de leur taille sur la résistance à l'écrasement ont été étudiées. Comme les sables égéens présentent des sphéricités et des émoussés peu variables, des essais d'écrasement ont aussi été réalisés sur cinq sables anatoliens. Une analyse par régression multiple a été réalisée et une équation proposée pour déterminer la résistance à l'écrasement des sables égéens. Les valeurs calculées sont apparues en bon accord avec les valeurs mesurées. On conclut que l'équation est suffisamment précise pour fournir des estimations utiles et peu coûteuses de la résistance à l'écrasement dans le contexte d'études préliminaires de site.

Mots clés Sables égéens · Sables anatoliens · Résistance à l'écrasement · Morphologie des particules · Sphéricité · Emoussé

Y. Erzin (✉) · M. G. Tiga
Department of Civil Engineering, Celal Bayar University,
45140 Manisa, Turkey
e-mail: yusuf.erzin@gmail.com; yusuf.erzin@bayar.edu.tr

A. Patel · D. N. Singh · K. Srinivas
Department of Civil Engineering,
Indian Institute of Technology Bombay,
Mumbai 400076, India
e-mail: apatel@iitb.ac.in

D. N. Singh
e-mail: dns@civil.iitb.ac.in

K. Srinivas
e-mail: srinivasciv@gmail.com

I. Yilmaz
Department of Geological Engineering,
Cumhuriyet University, 58040 Sivas, Turkey
e-mail: iyilmaz@cumhuriyet.edu.tr

Introduction

Most important engineering properties of sands, such as stress–strain/strength behavior, volume change and pore pressure developments and the variation in permeability, depend on the integrity of the particles or the amount of particle crushing (Lade et al. 1996). Crushing or particle breakage of soil grains occurs due to extremely high

stresses that may be generated during pile driving, construction of high earth or rock fill dams, laying foundations of offshore gravity structures, impact of projectiles, drilling at great depths for petroleum extraction etc. (e.g., Bishop 1966; Lo and Roy 1973; Miura and O-hara 1979; Hardin 1985; Zheng et al. 1990; Coop and Lee 1993). Extensive laboratory investigations have been conducted by researchers to assess the compression and crushing behavior of granular material (e.g., Miura et al. 1984; Hagerty et al. 1993; Morland et al. 1993; Ghosal and Self 1995; Mcdowell et al. 1996; Anand and Gu 2000; Nakata et al. 2001; Fedá 2002; Chuhan et al. 2003; Gupta et al. 2004; Bartake and Singh 2005, 2007). These studies demonstrate that some of the main factors which influence the crushing of grains are particle-size distribution, grain mineralogy, shape, hardness, density or void ratio, aspect ratio etc. (e.g. Miura et al. 1984; Hardin 1985; Fedá 2002; Chuhan et al. 2003).

Bartake and Singh (2007) have investigated the relationship between the crushing strength, particle size characteristics and G of granular material including sands, cenospheres and glass beads. Using these results, a generalized relationship for estimating its crushing strength has been proposed, Eq. 1, in which D_x corresponds to x percent finer fraction of the granular material.

$$\sigma_{CR}/G = \frac{20 \cdot D_{15} \cdot D_{45} \cdot D_{50} \cdot D_{80}}{(D_{10})^{1.6} \cdot D_{30} \cdot D_{60} \cdot (D_{90})^{1.2}} \quad (1)$$

Erzin and Yılmaz (2008) have investigated the influence of factors that affect the crushing resistance of three different Anatolian sands. They determined mineralogical, particle shape and size characteristics of the sands and conducted triaxial compression tests. It has been observed that particle crushing occurs in all shear tests. However, less particle crushing occurs in samples which contain higher proportions of quartz and lower proportions of calcite. Particle crushing is also observed to increase with increase in density.

A similar study has been undertaken using seven different Aegean sands collected from western Turkey (Fig. 1). The samples were tested for mineralogy, particle shape and size, and specific gravity. Crushing strength tests were performed on specimens with different aspect ratios ($H/d = 0.50, 0.75, 1.00, 1.25$ and 1.50) by employing the methodology proposed by Bartake and Singh (2007).

Aegean sands have a small range of sphericity and roundness. Thus, additional crushing tests were performed on five Anatolian sands, having different particle shapes and compositions, used by Erzin (2004), with a $H/d = 1.00$. It was found that Anatolian sands have higher crushing strength values than Aegean sands and again, higher proportions of quartz minerals gave high crushing strength values. Based on these results, a multiple regression

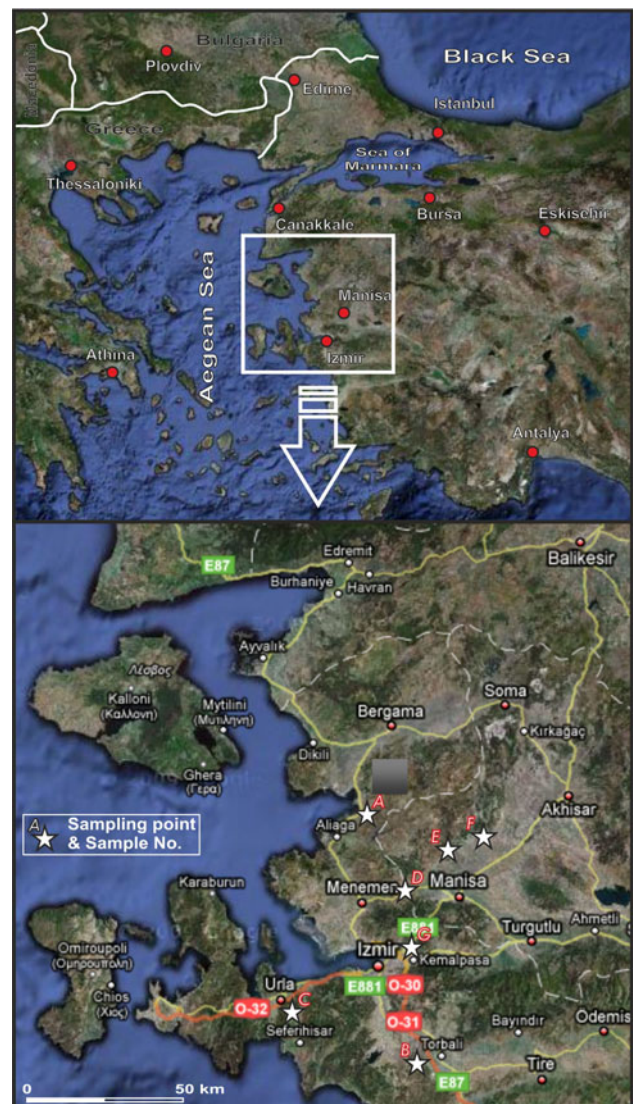


Fig. 1 Location map of the study area and the sampling points

analysis (MRA) equation was developed for predicting the crushing strength value of sands based on their mineralogical composition, particle shape, aspect ratio, specific gravity, coefficient of uniformity and coefficient of curvature. Coefficient of correlation (R), variance account for (VAF), root mean square error (RMSE) and scaled percent error (SPE) were calculated to check the prediction capacity of the equation and confirmed an acceptable accuracy for use as a rapid, inexpensive substitute for laboratory techniques in the preliminary stages of site investigations.

Investigation

The sands collected from the locations shown in Fig. 1 were air-dried and the fraction passing a 4.76 mm sieve (ASTM No. 4) was separated into representative sub-samples by passing through the riffle box.

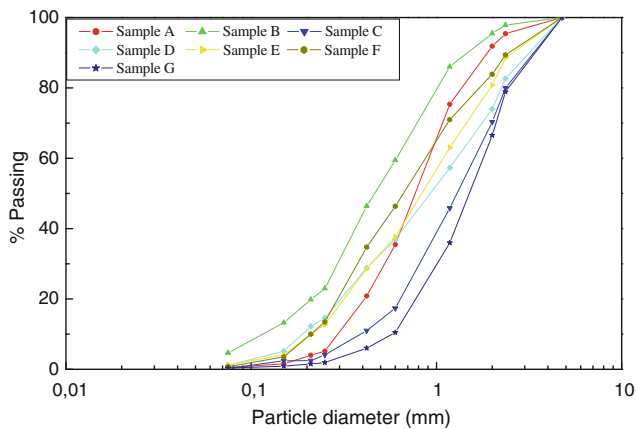


Fig. 2 Particle size distribution characteristics of the sand samples

In order to establish gradational characteristics of these sands, tests were performed in triplicate on each sample following the guidelines presented by ASTM D 422–63. The average values were used for developing the particle size distribution curve for the sample (Fig. 2). Table 1 presents the soil parameters and the specific gravity (G) which was established following ASTM D 5550.

X-ray diffraction analyses were carried out in two stages: whole-rock powder and oriented clay fraction. Semi-quantitative weight percentages of samples were calculated by using mineral intensity factors based on Gundogdu (1982). In this method, samples are mounted in the same way, and the characteristic peak intensities (I) of minerals are normalized to that of the reflection of dolomite. In other words, a K factor for each mineral, including clays with peaks between 19 and $20^{\circ}2\theta$, is determined as $K_{\text{dolomite}}/I_{\text{mineral}}$ in a 1:1 dolomite–mineral mixture by weight. Percentages of the minerals are calculated from the following equation:

$$a = (100K_a I_a) / (K_a I_a + K_b I_b + \dots + K_n I_n) \quad (2)$$

where a is the percentage of the mineral; and $K_{a,b,\dots,n}$ and $I_{a,b,\dots,n}$ are the K factor and intensity of each mineral identified. This method was preferred over other methods because it is simple to perform.

Table 1 Physical characteristics of the samples of Aegean sands

Sample	G	D_{10} (mm)	D_{30} (mm)	D_{60} (mm)	C_u	C_c	Unified soil classification
A	2.65	0.30	0.52	0.90	3.00	1.00	SP
B	2.17	0.13	0.30	0.60	4.62	1.15	
C	2.63	0.40	0.80	1.71	4.28	0.94	
D	2.61	0.20	0.45	1.31	6.55	0.77	
E	2.62	0.21	0.43	1.10	5.24	0.80	
F	2.62	0.21	0.38	0.90	4.29	0.76	
G	2.50	0.60	1.00	1.85	3.08	0.90	

According to the XRD results, quartz is the most prominent mineral in samples C to G, with feldspar, calcite and clay minerals found in small quantities. In sample A, higher proportions of feldspar and clay minerals were observed. Amorphous silicate minerals (85 %) were dominant in sample B (85 %) with 15 % quartz. The results are summarised in Tables 2, 3.

Particle shape analyses were carried out on 120 grains of each sand sample. The roundness (R_F) developed by Dobkins and Folk (1970), given by Eq. (3), and sphericity (S_R) described by Riley (1941), given by Eq. (4) were determined and the average values were considered as representative.

$$R_F = d_k/d_i \quad (3)$$

$$S_R = d_i/d_c \quad (4)$$

where d_k is the diameter of curvature of the sharpest corner, d_i is the diameter of the inscribed circle, and d_c is the diameter of the circumscribing circle (Fig. 3). A very well rounded particle has a maximum R_F of 1.0 while, an extremely angular particle has a value close to 0.0. A perfectly spherical particle has an S_R value of 1.0; smaller values mean departure from a spherical shape and the theoretical extreme is 0.0. The results are presented in Table 4.

Apparatus

In order to study the influence of H/d ($=0.5, 0.75, 1.0, 1.25$ and 1.5) on the measured crushing strength σ_{CR} of the samples, a laboratory test was set up as depicted in Fig. 4. This apparatus was fabricated by Bartake and Singh (2005) to determine crushing characteristics of the sands, cenospheres and glass beads. It consists of a 110 mm high stainless steel mold with an inner diameter of 33 mm and outer diameter of 51 mm, in which granular material can be filled to achieve a sample of the desired aspect ratio (i.e., height to diameter ratio, H/d) and density ρ . Two 32 mm diameter stainless steel pistons (top and bottom) were used for crushing the sample. A collar was provided at the bottom of the mold on which two removable stainless steel

Table 2 Whole rock powder diffraction analysis results (% fraction by weight) for the sand samples

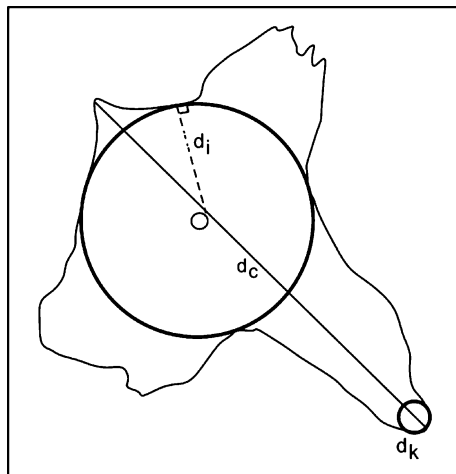
Sample	Location	Q	Fel	Ca	AS	Clay
A	Aliğa (I)	25	44	–	–	31
B	Menderes (I)	15	–	–	85	–
C	Seferihisar (I)	62	13	–	–	25
D	Menemen (I)	74	–	6	–	20
E	Üçpınar (M)	58	18	–	–	24
F	Karayenice (M)	52	27	–	–	21
G	Bornova (I)	40	16	16	–	28

I Izmir, *M* Manisa, *Q* quartz, *Fel* feldspar, *Ca* calcite, *AS* amorphous silicate

Table 3 Results of XRD oriented clay-size fraction diffraction analysis results (% by weight) for the sand samples

Sample	Location	S	I	K	Cl	Amrp.
A	Aliğa (I)	45	30	20	5	–
B	Menderes (I)	–	–	–	–	100
C	Seferihisar (I)	25	40	25	10	–
D	Menemen (I)	–	–	–	–	100
E	Üçpınar (M)	–	–	–	–	100
F	Karayenice (M)	–	–	–	–	100
G	Bornova (I)	–	–	–	–	100

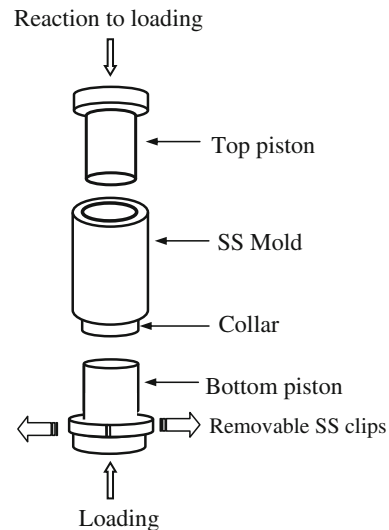
I Izmir, *M* Manisa, *S* smectite, *I* illite, *K* kaolinite, *Cl* chlorite, *Amrp* amorphous minerals (imogolite + allophanes)

**Fig. 3** Definitions of angularity and sphericity (Dobkins and Folk 1970)

clips of thickness 10 mm can be fixed. These clips were removed before commencing the test to achieve loading of the sample from both the ends.

Table 4 Results of the particle shape analyses on the sand samples

Sample	R_F	S_R
A	0.15	0.60
B	0.14	0.59
C	0.14	0.59
D	0.15	0.60
E	0.14	0.58
F	0.17	0.64
G	0.17	0.60

**Fig. 4** The test setup used for determining crushing strength of sands

Methodology

A 10 kN load cell compression testing machine supplied by Humboldt, USA was employed in this study. The tests were performed at a strain rate of 1.25 mm/min (Karner et al. 2004). The load cell was attached to a digital readout unit to record the load (P) transmitted to the sample at 10 s intervals. Prior to loading of the sample, silicon grease was applied on the two pistons to minimize the side friction. The sample was poured into the mold by adopting the rainfall technique (i.e., using a funnel and maintaining a constant height of fall) to achieve a certain H/d .

Results and discussion

Typical load-deformation (P - δ) characteristic curves were developed for Samples A to G, corresponding to different H/d ratios (=0.5, 0.75, 1.0, 1.25 and 1.5). The results pertaining to sample C (with $H/d = 1.0$) are presented in Fig. 5. After an initial elastic response (depicted by portion

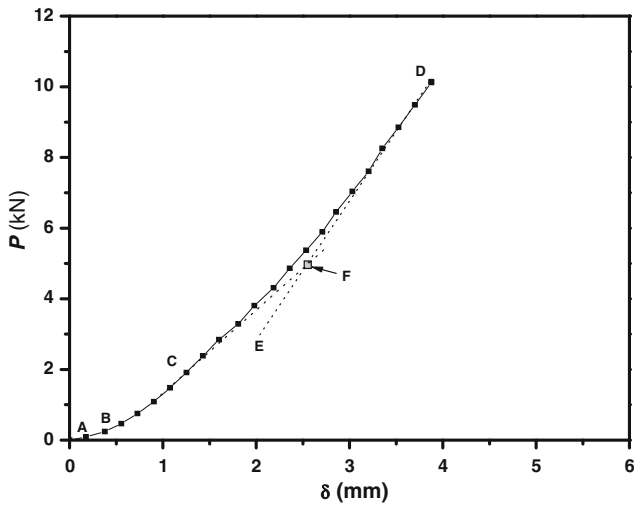


Fig. 5 Typical load-deformation characteristics of the Sample F ($H/d = 1.0$)

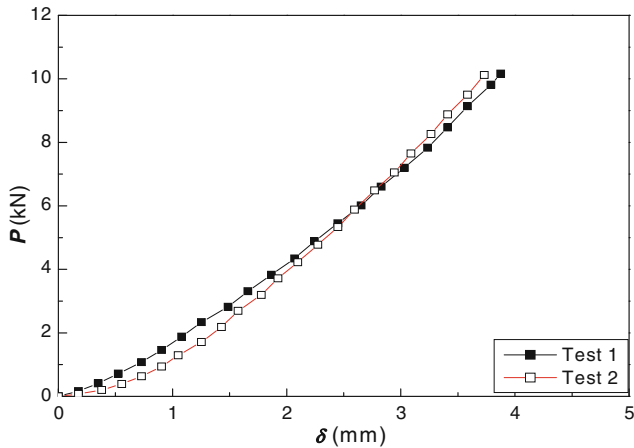


Fig. 6 Reproducibility of the load-deformation characteristics of Sample A ($H/d = 1.0$)

AB of the P - δ characteristics), rearranging and repacking of the particles starts (depicted by portion BC). Point C corresponds to the point on the P - δ characteristics with the maximum curvature. Beyond point C, sands lose their integrity, hence a tangent drawn to the P - δ characteristics at point C intersects its upper linear portion (represented as DE) at F, which would yield σ_{CR} . As depicted in the figure, the crushing load of the sample is 5.0 kN, which corresponds to $\sigma_{CR} = 6.6$ MPa.

To check the reproducibility of the P - δ characteristics, two tests were performed on Sample A by maintaining $H/d = 1$. The results are depicted in Fig. 6 which indicates the two trials yield very similar trends.

The influence of H/d on σ_{CR} was also investigated. As an example, the P - δ characteristics of Samples B and G are given in Figs. 7, 8, respectively. By employing the

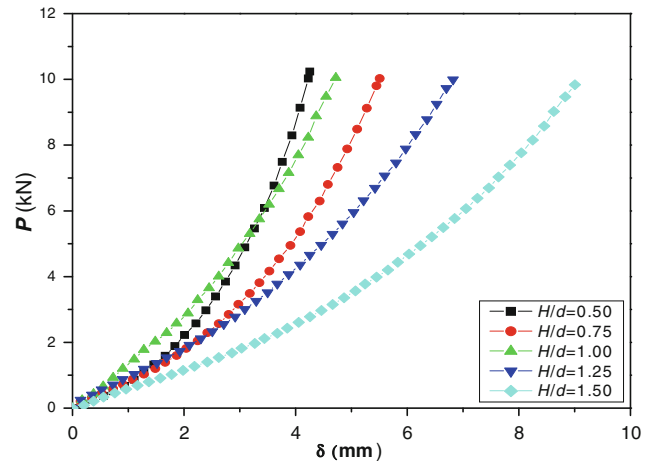


Fig. 7 Typical load-deformation characteristics of Sample B

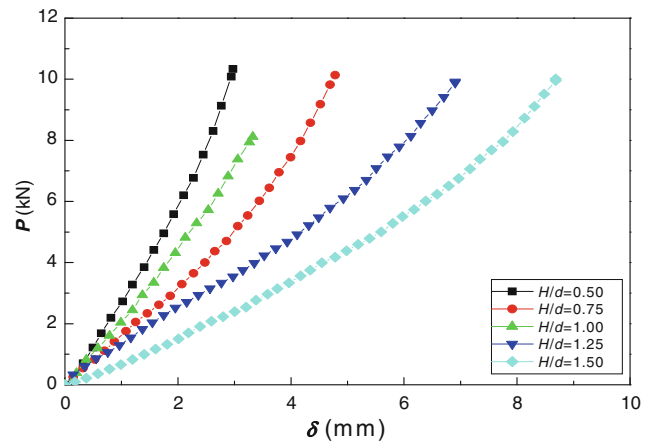


Fig. 8 Typical load-deformation characteristics of Sample G

methodology in Fig. 5, the σ_{CR} of Samples A to G was computed as shown in Fig. 9. It can be seen that initially, σ_{CR} increases non-linearly with H/d and thereafter it attains a nearly constant value. The transition point between these two trends corresponds to $H/d = 1$. Hence, for determining the σ_{CR} of the Aegean sands, tests should be conducted with $H/d > 1$.

A comparison of the σ_{CR} values of Samples A to G (for $H/d = 0.5$) indicates that σ_{CR} is highest (7.2 MPa) for Sample D. Similar trends were observed for other H/d ratios. This can be attributed to the fact that Sample D contains the highest proportion of quartz (refer Table 2), and has the highest C_u value (=6.55, refer Table 1), supporting the work of Erzin and Yilmaz (2008).

It is of note that for $H/d = 0.5, 0.75, 1.0, 1.25$ and 1.5 , higher σ_{CR} values were obtained for Sample F compared with Sample G which has a similar R_F and S_R . However, Sample F has a higher C_u (Table 1) and higher proportions of quartz and feldspar with lower proportions of clay

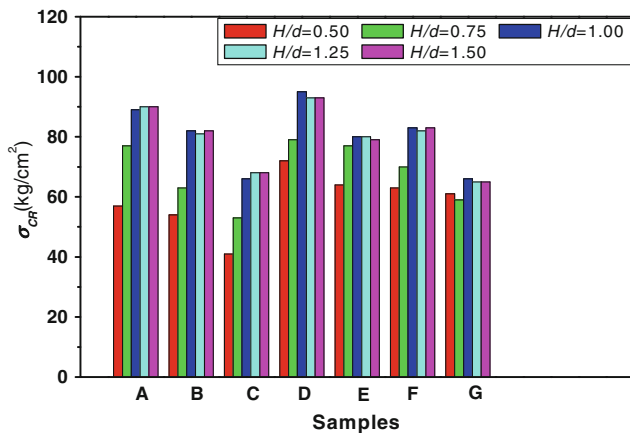


Fig. 9 A comparison of crushing strength of different sand samples

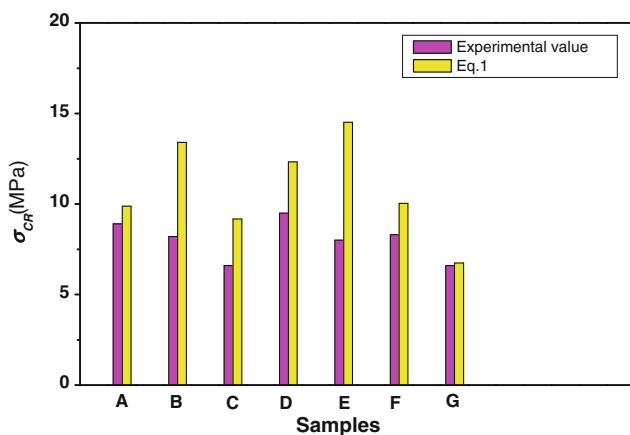


Fig. 10 A comparison of the measured and predicted crushing strengths of different sand samples ($H/d = 1.0$)

minerals compared to Sample G (Table 2). In addition, Sample G contains 16 % calcite.

In addition, the σ_{CR} for Samples A to G were computed from Eq. 1 and compared with the experiment results for $H/d = 1.0$ (Fig. 10). It can be seen that Eq. 1 yields higher σ_{CR} results; the lowest difference (0.15 MPa) being obtained for Sample G and the highest (6.52 MPa) for sample E. This discrepancy can be attributed to the fact that the particle size distribution characteristics on which Eq. 1 is based, is not the only factor which influences the crushing strength of the Aegean sands but particle shape, mineralogical composition and aspect ratio should also be taken into account.

As the Aegean sands used in this study have a small range of sphericity and angularity (Table 4), crushing strength tests ($H/d = 1.0$) were also performed on five Anatolian sands with different particle shapes and compositions, as used by Erzin (2004); see Table 5. X-ray diffraction analyses were carried out on two of the Anatolian sand samples (samples H and J) while for the

other samples the results were taken from Erzin and Yilmaz (2008). The whole rock powder diffraction analysis results (% fraction by weight) for the Anatolian sand samples is given in Table 6 and the particle shape analyses in Table 7 (from Erzin and Yilmaz 2008).

The crushing strength of the Aegean and Anatolian sands ($H/d = 1.0$) are compared in Fig. 11. Although the σ_{CR} values of Anatolian sands are higher than those for Aegean sands, again the proportion of quartz is significant.

A model based on multiple regression analysis (MRA) was developed to predict σ_{CR} based on mineralogical composition, particle shape, aspect ratio, specific gravity, coefficient of uniformity and coefficient of curvature, using SPSS 8.0.0 (Statistical Package for the Social Sciences). The experimentally obtained G , R_F , S_R , C_w , C_c , H/d and the proportions of quartz, feldspar, calcite and clay minerals (Q , F , Ca and Clay respectively) were used and the following equation was obtained.

$$\begin{aligned} \sigma_{CR}/G = & 5.4 + 1.0 \cdot R_F - 6.4 \cdot S_R - 0.6 \cdot C_u \\ & + 1.9 \cdot C_c + 0.9H/d + 0.8 \cdot Q + 0.8 \cdot F \\ & + 0.6 \cdot Ca - 0.2 \cdot \text{Clay} \end{aligned} \quad (5)$$

The computed σ_{CR} values from Eq. (5) are compared vis-à-vis experimentally obtained σ_{CR} values in Fig. 12. The solid diagonal line in Fig. 12 represents a perfect prediction line. The lower line represents a 100 % over-prediction bound and the upper line represents a 50 % under prediction bound. Approximately 80 % of the predictions fall onto or are very close to the 1:1 line and all of the predictions fall between these two prediction lines. The high coefficient of correlation ($R = 0.96$) indicates a strong correlation between the computed and measured σ_{CR} values. Variance (VAF), represented by Eq. (6), and the root mean square error (RMSE) represented by Eq. (7), were also computed (Gokceoglu 2002; Erzin 2007; Erzin et al. 2008).

$$VAF = \left[1 - \frac{\text{var}(y - \hat{y})}{\text{var}(y)} \right] \times 100 \quad (6)$$

$$RMSE = \sqrt{\frac{1}{N} \sum_{i=1}^N (y_i - \hat{y}_i)^2} \quad (7)$$

where var denotes the variance, y is the measured value, \hat{y} is the predicted value, and N is the number of the sample. If VAF is 100 % and RMSE is 0, the model is treated as excellent. Values of VAF and RMSE were found as 91.9 % and 1.7 MPa.

In addition to the performance indices, a graph between the scaled percent error (SPE), given by Eq. (8), as employed by Kanibir et al. (2006), and cumulative frequency was also drawn in Fig. 13 to show the performance of the models developed.

Table 5 Physical characteristics of the samples of the Anatolian sands (Erzin 2004)

Sample	G	D_{10} (mm)	D_{30} (mm)	D_{60} (mm)	C_u	C_c	Unified soil classification
H	2.64	0.20	0.59	1.16	5.80	1.50	SP
I	2.70	0.21	0.29	0.37	1.76	1.08	
J	2.68	0.23	0.39	0.80	3.48	0.83	
K	2.64	0.33	0.39	0.41	1.24	1.12	
L	2.70	0.21	0.33	0.46	2.19	1.13	

Table 6 Whole rock powder diffraction analysis results (% fraction by weight) for the Anatolian sand samples

Sample	Q	Fel	Ca	Clay
H	45	40	–	15
I	37	27	36	–
J	40	40	–	20
K	94	3	3	–
L	58	26	11	–

Q quartz, Fel feldspar, Ca calcite

Table 7 Results of the particle shape analyses on the Anatolian sand samples (Erzin 2004)

Sample	R_F	S_R
H	0.25	0.78
I	0.33	0.80
J	0.21	0.78
K	0.30	0.77
L	0.34	0.79

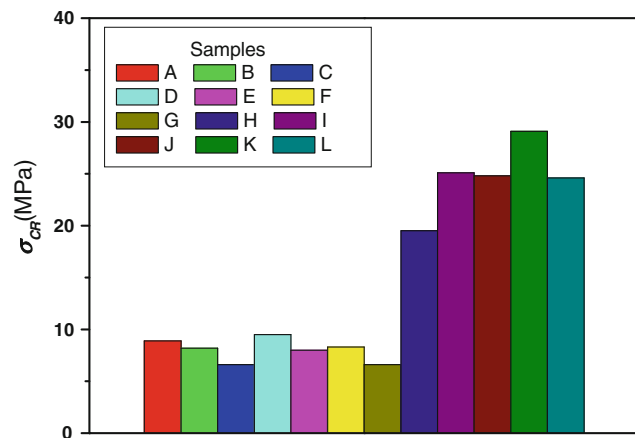


Fig. 11 A comparison of crushing strength of sand samples A to L

$$SPE = \frac{((\sigma_{CR})_p - (\sigma_{CR})_m)}{((\sigma_{CR})_m)_{\max} - ((\sigma_{CR})_m)_{\min}} \quad (8)$$

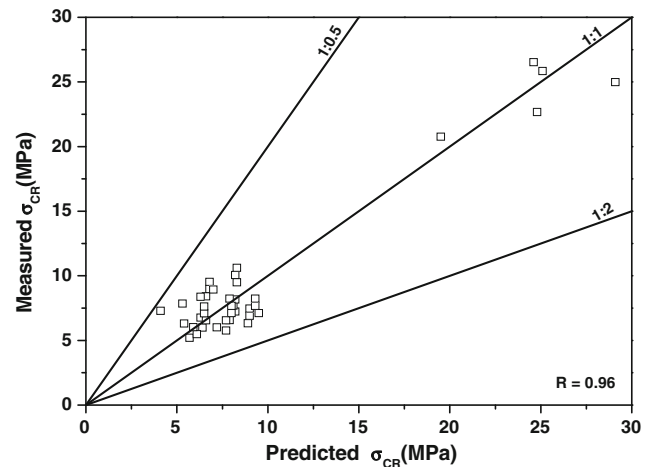


Fig. 12 Comparison of experimentally obtained and computed values of σ_{CR} for Aegean and Anatolian sands

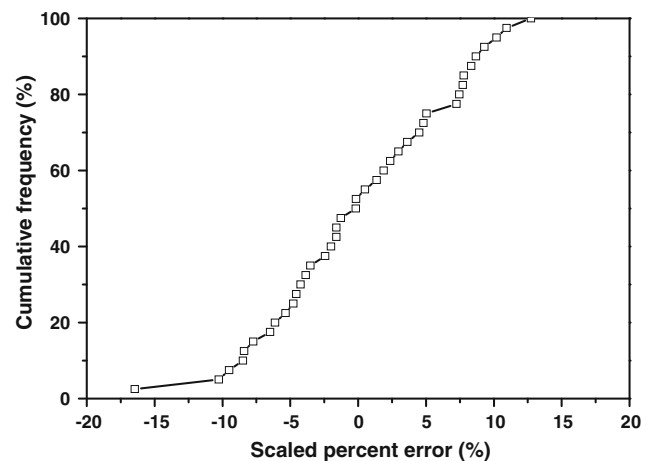


Fig. 13 The relationship between the scaled percent error and cumulative frequency

where $(\sigma_{CR})_p$ and $(\sigma_{CR})_m$ are the predicted and measured crushing strengths; and $[(\sigma_{CR})_m]_{\max}$ and $[(\sigma_{CR})_m]_{\min}$ are the maximum and minimum measured crushing strengths, respectively. As seen from Fig. 13, about 90 % of the crushing strengths predicted from the MR model are ± 10 % of the SPE.

Conclusions

In this study, the influence of factors affecting the crushing strength of Aegean sands has been investigated. Samples from seven different locations were analyzed for mineralogical, particle shape and size, specific gravity and crushing strength tests and the influences of aspect ratio, particle composition, particle shape and size on the crushing strength were examined. It has been observed that the crushing strength, σ_{CR} , initially increases non-linearly with H/d and thereafter attains a nearly constant value for each sample. The highest σ_{CR} was obtained for the sample with the highest C_u value and containing the highest proportion of quartz. Due to the fact that Aegean sands used in this study have a small range of sphericity and angularity, crushing strength tests were also performed on five Anatolian sands for $H/d = 1.0$. The σ_{CR} values of Anatolian sands are found to be higher than those for Aegean sands but the significant factor was again the proportion of quartz.

An MRA equation was developed for predicting the σ_{CR} value of sands based on their mineralogical composition, particle shape, aspect ratio, specific gravity, coefficient of uniformity and coefficient of curvature and the applicability of the equation demonstrated using R , VAF and RMSE.

It is concluded that for these sands the proposed equation is sufficiently accurate for use as a rapid, inexpensive substitute for laboratory techniques in the preliminary stages of site investigations.

References

- Anand L, Gu C (2000) Granular materials: constitutive equations and strain localization. *J Mech and Phys Solids* 48:1701–1733
- ASTM D 422-63 (1994) Standard test method for particle size analysis of soils, *Annual Book of ASTM Standards*, ASTM, West Conshohocken, PA, USA, 04.08, 10–16
- ASTM D 5550 (2001) Standard test method for specific gravity of soil solids by gas pycnometer, *Annual Book of ASTM Standards*, ASTM, West Conshohocken, PA, USA, 04.08
- Bartake PP, Singh DN (2005) Determination of crushing strength of cenospheres. *J ASTM Int* Published online, 2(7):9 pp
- Bartake PP, Singh DN (2007) A generalized methodology for determination of crushing strength of granular materials. *Geotech Geol Eng* 25(2):203–213
- Bishop AW (1966) The strength of soils as engineering materials. *Geotechnique* 16(2):91–128
- Chuhan FA, Kjeldstad A, Bjorlykke K, Hoeg K (2003) Experimental compression of loose sands: relevance to porosity reduction during burial in sedimentary basins. *Can Geotech J* 40:995–1011
- Coop MR, Lee IK (1993) The behaviours of granular soils at elevated stresses. In *Predictive soil mechanics*, Thomas Telford, pp 186–199
- Dobkins JE and Folk RL (1970) Shape development on Tahiti-Nui. *J Sediment Petrol* 40:1167–1203
- Erzin Y (2004) Strength of different Anatolian sands in wedge shear, triaxial shear and shear box tests. Ph.D. thesis, Middle East Technical University, Ankara, Turkey, 227 pp
- Erzin Y (2007) Artificial neural networks approach for swell pressure versus soil suction behavior. *Can Geotech J* 44(10):1215–1223
- Erzin Y, Yilmaz I (2008) A case study of crushing resistance of Anatolian sands at lower and higher density. *Bull Eng Geol* 67:71–77
- Erzin Y, Rao BH, Singh DN (2008) Artificial neural network models for predicting soil thermal resistivity. *Int J Therm Sci* 47:1347–1358
- Feda J (2002) Notes on the effects of the grain crushing on the granular soils behaviour. *Eng Geol* 63:93–98
- Ghosal S, Self AS (1995) Particle size density relation and cenosphere content of coal fly ash. *Fuel* 74(4):522–529
- Gokceoglu C (2002) A fuzzy triangular chart to predict the uniaxial compressive strength of Ankara agglomerates from their petrographic composition. *Eng Geol* 39–51
- Gundogdu, N., 1982. Geological, mineralogical and geochemical investigation of the Neogene aged Bigadic, sedimentary basin. Ph.D. thesis, Hacettepe University, Ankara, Turkey, 386 pp. (in Turkish)
- Gupta N, Woldesenbet E, Mensah P (2004) Compression properties of synthetic foams: effect of cenosphere radius ratio and specimen aspect ratio. *Compos Part Appl Sci Manufact* 35:103–111
- Hagerty MM, Hite DR, Ulrich CR, Hagerty DJ (1993) One-dimensional high-pressure compression of granular media. *J Geotech Eng ASCE* 119(1):1–18
- Hardin BO (1985) Crushing of soil particles. *Journal of Geotechnical Engineering*, ASCE 111(10):1177–1192
- Kanibir A Ulusay R Aydan Ö (2006) Liquefaction-induced ground deformations on a lake shore (Turkey) and empirical equations for their prediction. *IAEG2006*, paper 362
- Kamer, S.L., Chester, F.M., Kronenberg, A.K., Hajash, Jr A. 2004. Laboratory deformation of granular sand: implications for the burial of clastic rocks. *AAPG Bulletin*, 1–57
- Lade PV, Yamamuro JA, Bopp PA (1996) Significance of particle crushing in granular materials. *J Geotech Eng ASCE* 122(4):309–316
- Lo KY, Roy M (1973) Response of particulate materials at high pressure. *Soils Found* 13(1):61–76
- McDowell GR, Bolton MD, Robertson D (1996) The fractal crushing of granular materials. *J Mech Phys Solids* 44(12):2079–2102
- Miura N, O-hara S (1979) Particle crushing of a decomposed granite soil under shear stress. *Soils Found* 19(3):1–14
- Miura N, Murata H, Yasufuku N (1984) Stress-strain characteristics of sand in a particle crushing region. *Soils Found* 24(1):77–89
- Morland LW, Sawicki A, Milne PC (1993) Uni-axial compression of granular material. *J Mech Phys Solids* 41(1):1755–1779
- Nakata Y, Hyodo M, Hyde AFL, Kato T, Murata H (2001) Microscopic particle crushing of sand subjected to high pressure one-dimensional compression. *Soils Found* 41(1):69–82
- Riley NA (1941) Projection sphericity. *J Sediment Petrol* 1:94–97
- Zheng J, Wong TF, Yanagidani T, Davis DM (1990) Pressure induced microcracking and grain crushing in Berea and Boise sandstone-acoustic emission and quantitative measurements. *Mechanics Mater* 9:1–5